

STRUCTURAL PARAMETERS AND COMPARATIVE ANALYSIS OF THE PERFORMANCE OF FOUR BEETLE ELYTRON PLATE WALLS

Yinsheng LI¹, Liping HU¹, Jinxiang CHEN^{1✉}, Canjun SHENG²

¹Key Laboratory of Concrete and Prestressed Concrete Structures of the Ministry of Education, Southeast University, Nanjing, China

²Suzhou Bo Guan Yue Qu Intelligent Equipment co. Ltd, Suzhou, China

Article History:

- received 13 January 2022
- accepted 29 June 2023

Abstract. This article presents the characteristics of four straw-filled beetle elytron plate (BEPsc) nonload-bearing walls, with their thermal and mechanical properties ascertained by the finite element method, focusing on structural parameters reported in previous studies and further optimized in this paper. The results are as follows: 1) The sequence of the four models' mechanical and thermal insulation properties with the reported structural parameters is given. The mechanical properties are mainly affected by the core layer's out-of-plane bending moment of inertia I_x . The insulation capability is mainly governed by the minimum cross section of the core concrete. Based on this result, a BEP with nonuniform cross-sectional honeycomb walls is proposed. 2) Further optimization is conducted on the two models with the weakest mechanical and thermal properties. The I-beam beetle elytron plate (IBEPsc) is proven most suitable for nonload-bearing walls. The potential for end-trabecular beetle elytron plate (EBEPsc) in hollow floors is expected. 3) As biomimetic models emerge constantly, it is of great significance to conduct parallel comparisons between new and old models to determine their performance levels and advantages. This paper provides an example for selecting suitable BEPs for applications and an inspiration for more work on screening outstanding biomimetic models.

Keywords: beetle elytron plate, nonload-bearing walls, maximum principal tensile stress, heat transfer coefficient, biomimetic optimization.

✉Corresponding author. E-mail: chenjpaper@yahoo.co.jp

1. Introduction

Energy consumption during construction in China accounts for 30% to 50% of the total energy consumption, three times that of developed countries (Jin, 2019). Moreover, the heat transference from the maintenance structure accounts for 70~80% of the total heat loss of the building. Therefore, improving the insulation performance of the envelope is the key to achieving building energy savings (Wu et al., 2015). For this reason, many scholars in China have conducted research studies on exterior wall insulation materials (Wu et al., 2015; Qing & Zhang, 2016; Bao et al., 2017). Among them, the new prefabricated wall with crop straw as the raw material has considerable significance. To date, China's annual straw production has reached 1 billion tons (Li et al., 2018), but 30% of straw is burned directly in the field (Chen et al., 2019a). Thus, straw walls can not only make full use of abundant straw resources but also effectively avoid the environmental pollution caused by direct burning. In recent years, the enhanced envelope in-

ulation requirements have thickened the insulation layer with materials such as asbestos and polystyrene in traditional exterior walls. New challenges have emerged in fire prevention, insulation layer anchorage, and construction cost control. Therefore, the significance of developing a new type of straw thermal insulation wall, which can mitigate the above series of problems, has become salient. In fact, several years ago, biomimetic sandwich panels with mechanical cement-based straw cores were proposed as an important development direction (Yu et al., 2021; Chen et al., 2021a). Subsequently, four beetle elytron plate (BEP) nonload-bearing walls were proposed, whose mechanical and self-insulating properties are suitable for buildings highly affected by typhoons in the coastal areas of eastern and southern China (Zhang et al., 2019, 2020a; Hu, 2021; Hu et al., 2021).

These four wall plates evolved from BEPs inspired by the structure of an *A. dichotomus* elytron (Figures 1a and

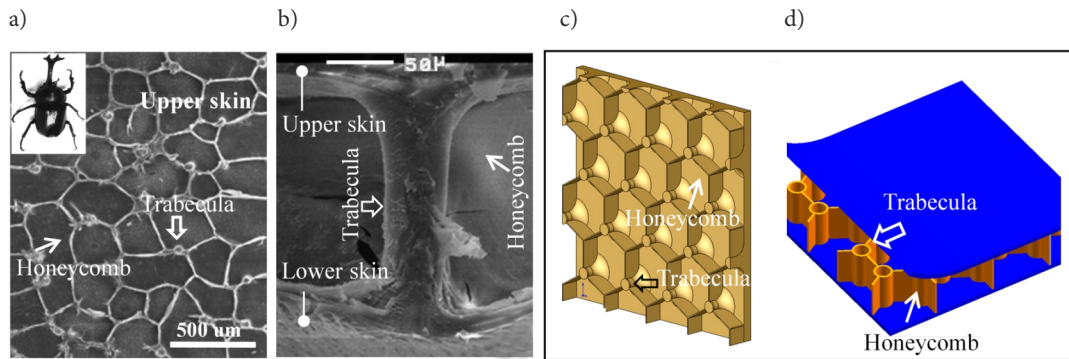


Figure 1. The development of beetle elytron plates: a – The internal structure of the elytron, with the adult *A. dichotoma* beetle in the corner; b – The trabecula in the elytron (Hu, 2021; Hu et al., 2021; Song et al., 2021); c, d – Two different BEPsc (Chen et al., 2002, 2012, 2019b; Chen, 2018)

1b) and were proposed by the corresponding author of this paper (Figures 1c and 1d) (Chen et al., 2002, 2012, 2019b; Chen, 2018). As shown in Figure 2, among them, the first straw sandwich concrete beetle elytron plate has a simple structure with lateralized solid columns (Figure 2a, originally denoted SCBEP (Zhang et al., 2019) and denoted TBEPsc in this paper). The columns of the TBEPsc are imitated from the protein columns of the beetle forewing, arranged in a uniform lattice pattern, with chamfered edges at the junction with the panels. It has been demonstrated that their mechanical and insulation properties fulfill the fundamental requirements of self-insulating prefabricated wall structures. However, BEPsc with honeycomb walls have stronger mechanical properties than TBEPsc (Zhang et al., 2017; Xu et al., 2019). To develop a better self-insulating straw sandwich panel, the second model, called the vertical trabeculae beetle elytron plate (VBEPsc), with honeycomb walls and columns verticalized was proposed, as shown in Figure 2b (Zhang et al., 2020a). As research progressed, BEPsc with hollow columns tended to show better mechanical properties. Therefore, an attempt to replicate the biological original structure more realistically has led to the proposal of the wall-end column beetle elytron plate (EBEPsc (Hu, 2021), Figure 2c). In addition, the low functionality for bending resistance of the vertical column located in the middle of the thin wall was realized when reviewing the VBEPsc. Accordingly, by canceling the unnecessary columns and adopting an I-shaped structure, an I-beam beetle elytron plate¹ (IBEPsc, Figure 2d) was proposed (Hu et al., 2021).

In terms of mechanical performance, all of the aforementioned BEPsc can meet the requirements for load-bearing capacity and insulation performance after optimization. As for the manufacturing process, we are trying to

develop internal mold preparation techniques specific to each BEPsc. This technique connects and fixes inner molds filled with straw to an outer formwork, and then prepares the BEPsc by pouring concrete. Among the four BEPsc, TBEPsc, VBEPsc, and IBEPsc are relatively easy to prepare, while EBEPsc is the most challenging due to its core area being divided into multiple discontinuous intervals by the columns and honeycomb walls. It requires the most types and quantities of internal molds, and the hexagonal arrangement greatly increases the labor required for installing the internal molds during the preparation process.

Although the aforementioned achievements have been made, the development and optimization process of the aforementioned four beetle-inspired panels only elaborated on their respective performances. The optimized panel thicknesses are also not the same, making it difficult to conduct a systematic parallel comparison based on existing research, and difficult to accurately grasp the advantages and characteristics of each BEPsc, as well as their respective applicable engineering scenarios. At the same time, with the deepening of research, shortcomings in previous studies have also been noted, and corresponding measures for further optimization and improvement have been proposed. In fact, similar problems can also be found in biomimetic studies of beetle elytron 3D structures and biomimetic models reported by peers. In addition, misunderstandings or misrepresentations of biological structures buried in some investigations have worsened the situation. And there are few studies that discuss whether newly proposed models are truly stronger and more efficient than existing models in their respective applications. In this context, instead of the constant reports of nominal new models, it is better to characterize or identify the effectiveness of the existing biomimetic structures, which appear to be as important as the former. This article aims to reveal the characteristics of four types of beetle boards and provide a simpler and more systematic engineering application basis for clarifying the selection principles of BEPsc and easily predicting their insulation properties. In this paper, four proposed models, with the optimal structural parameters reported in previous studies and two additional optimized models, were unified with respect to thickness. A

¹ According to the original definition of beetle elytron plate – a sandwich board with a core trabecula layer or a combination of trabecular and honeycomb walls – this structure could not be called a beetle elytron plate. However, this “I-beam” structure is proposed again from the evolution of the biomimetic structure. In this sense, the optimized structure parameters are influenced by the beetle elytron structure. For convenience, it has been denoted as “I-beam beetle elytron plate” in the previous papers as well.

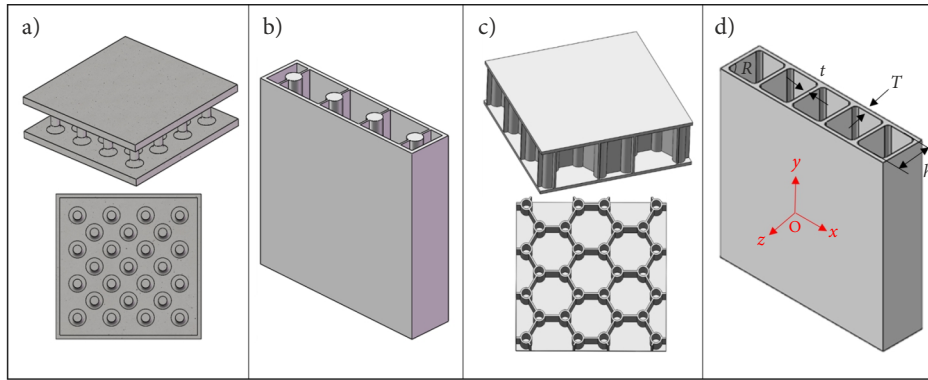


Figure 2. The evolutionary process of straw-filled concrete beetle elytron plates and their 3D model: a – TBEPsc (Zhang et al., 2019); b – VBEPsc (Zhang et al., 2020a); c – EBEPsc (Hu, 2021); d – IBEPsc (Hu et al., 2021)

comprehensive analysis of their mechanical and thermal insulation properties was conducted. This work is expected to provide a reference for the selection of suitable BEPs in engineering and inspire similar systematic and comprehensive evaluation studies.

2. Structural parameters of the model and the analysis method

2.1. Structural parameters of the four models

As discussed in the introduction, four BEPs were proposed, as shown in Figure 2, and their structure parameters were optimized by our group. In the previous study, we summarized the structural parameters that may affect the performance of BEPsc (listed in Table 1, with the meanings of each parameter shown in Figure 3), and revealed the relationship between the mechanical and insulation performance of the BEPsc with varying values through finite element analysis. With the expected application scenario of passive housing in southeastern China, optimal parameter values were proposed to achieve the best mechanical and insulation performance under assumed load conditions (mechanical performance includes maximum stress and maximum deflection, and insulation performance includes heat transfer coefficient). The complete optimization process and details are available in the references (Zhang et al., 2019, 2020a; Hu, 2021; Hu et al., 2021). In the comparative study of this article, the core structural parameters of the four BEPsc are still set to the optimal

values in the original paper and listed in Table 1. According to the original text, the four types of BEPs have two different thicknesses: 200 mm and 240 mm. In this comparative study, the 200 mm thick BEPs would be at a disadvantage. To avoid underestimating its performance level among the four BEPs due to its thinner thickness, this paper has standardized the plate thickness. Therefore, the geometric dimensions are as follows: BEP thickness = 240 mm, core layer height = 200 mm, and dimensions of the full-size model = 3×3 m. As these parameters were not proposed through biomimetic optimization, but rather pre-set by the author based on common engineering dimensions before parameter optimization, small variations in these parameters have little effect on the core structure characteristics. The comparison results can still reveal the performance ranking of the four BEPs structures.

2.2. Analytical conditions

Abaqus is used for finite element analysis. Limit requirements, which are similar to those in a previous paper (Hu, 2021), were proposed to ensure that the BEPs meet the requirements of load-bearing capacity, serviceability, and self-insulation. These requirements include the following: Capacity requirement: maximum compressive stress $\sigma_c \leq 4.29$ MPa; serviceability requirements: maximum tensile stress $\sigma_t \leq 1.43$ MPa (no cracking) and the maximum deflection perpendicular to the panel $\delta \leq 12$ mm; and Self-insulation requirement: the heat transfer coefficient of the wall in hot summer and warm winter areas $K_r \leq$

Table 1. Optimal parameters of BEPs (Zhang et al., 2019, 2020a; Hu, 2021; Hu et al., 2021)

	Column spacing L (mm)	Trabecular inner/outer radius R/r (mm)	Corner radius r_c (mm)	Honeycomb wall thickness t (mm)	Amount of vertical trabecula/honeycomb walls n_v/n_h	Core concrete area A_c (m ²) ^a	Core concrete volume V_c (m ³)
TBEPsc	240	25/0	50	–	–	0.92	0.24
VBEPsc ^b	–	40/0	–	10	12/14	0.83	0.32
EBEPsc	270	64/44	–	20	–	1.30	0.26
IBEPsc ^b	–	–	20	20	0/14	1.19	0.25

Notes: ^a The core concrete area is the area of the minimum section of the core concrete; ^b The full-scale models of VBEPsc and IBEPsc consist of three slats, and the two edge panels separating them are also counted in n_h .

$1.5 \text{ W}\cdot\text{m}^{-2}\cdot\text{K}^{-1}$. Table 2 shows the material properties used in the analysis. The mechanics and heat transfer analytical conditions, which were generally the same as in the previous solution (Hu 2021; Hu et al., 2021), are briefly described below.

2.2.1. Mechanical analysis

The BEP nonload-bearing walls will be used as the external wall, which mainly bears wind load, resulting in out-of-plane bending. In the analysis of mechanical properties, the stress distribution and magnitude of the wall under out-of-plane bending will be considered. The magnitude of the wind load is relatively small, and the external wall should have no crack and small deflection to meet the serviceability requirements (Zhang et al., 2020a). Thus, only the elastic constitutive model was considered for the concrete. The elastic modulus of the straw is much smaller than that of the concrete, and the load is mainly borne by the concrete. The straw was also analyzed as an elastic material. The C3D8I unit was used in the simulations. The mesh size for concrete was 20 mm and that for straw was appropriately increased, up to 100 mm. The wind load and self-weight were considered. The gravitational acceleration constant was 9.8 N/kg. The standard value of the wind load was 2.35 kPa. It was calculated as follows (Hu, 2021): the wind speed was assumed to be $v = 40 \text{ m/s}$, and the standard value of the wind load was calculated by $\omega_k = \beta_{sz}\mu_{s1}\mu_z\omega_0 = 2.35 \text{ kN/m}^2$, where $\beta_{sz} = 1.73$, $\mu_{s1} = 1.0$, $\mu_z = 1.36$, $\omega_0 = v^2 / 1600 = 1 \text{ kN/m}^2$. When analyzing the wall panel stiffness, the deflection was calculated using the standard values of wind load and ver-

tical load. When the bearing capacity analyses were performed, the standard values were multiplied by 1.4 (Standardization Administration of China, 2012). Tie constraints were built between the filled straw and concrete frame. To ensure safety redundancy, flexible connections are assumed between the BEPsc nonload-bearing wall and the load-bearing components. Guiding by the assumption, the boundary conditions were considered as follows: the grouted bottom of the wall was regarded as fixed support; the restraint of the main structure on both sides of BEPsc is equivalent to the sliding hinge support restraint, i.e., only the restraint of in-plane lateral displacement is considered and the BEPsc is allowed to rotate out-of-plane. Additionally, only the horizontal displacement was restrained on the upper end to generate the deformation caused by self-weight (Zhang et al., 2019). Figures 4a, 4b, and 4c show the boundary conditions and meshing of the mechanical analysis model using VBEPsc as an example.

2.2.2. Heat transfer analysis

The heat transfer analysis of the wall is aimed at obtaining the heat transfer coefficient of the wall under steady-state heat transfer. The finite element analysis is still performed in Abaqus to calculate the heat flow through the wall under the temperature difference between the indoor and outdoor surfaces. For the grid, the DC3D8 unit was used, and the mesh size was 20 mm. The walls are intended to be used in areas such as Jiangsu, China, where straw resources are abundant and its building climate demarcation is classified as hot summer and warm winter areas (Standardization Administration of China, 2015). The average in-

Table 2. Material properties of concrete and straw (Zhang et al., 2019, 2020a; Hu, 2021; Hu et al., 2021)

Material	Density	Young's modulus	Poisson's ratio	Heat conductivity coefficient	Specific heat
Unit	$\text{kg}\cdot\text{m}^{-3}$	MPa	–	$\text{W}\cdot\text{m}^{-1}\text{K}^{-1}$	$\text{J}\cdot\text{kg}^{-1}\text{K}^{-1}$
Concrete	2380	30000	0.20	1.28	960
Straw plate	250	0.70	0.18	0.06	2000

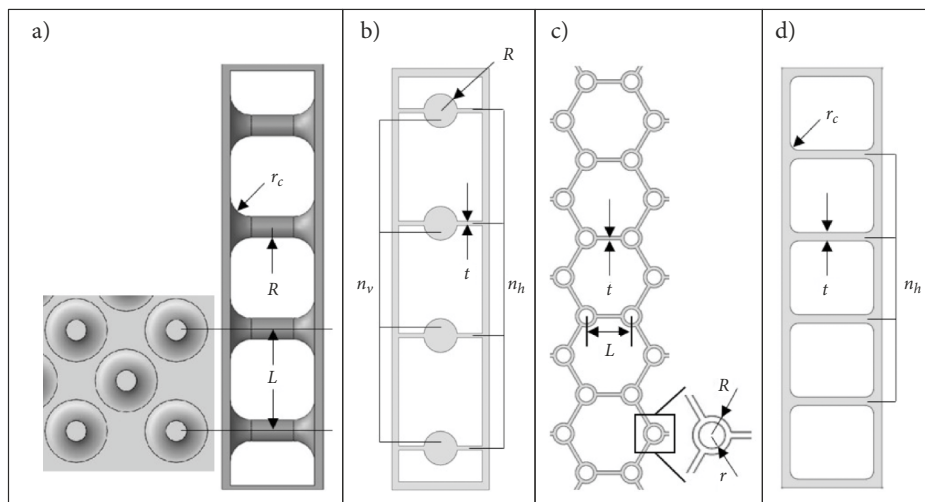


Figure 3. Inner structure parameters on the representative sections of beetle elytron plates: a – TBEpsc; b – VBEPsc; c – EBEPsc; d – IBEPsc

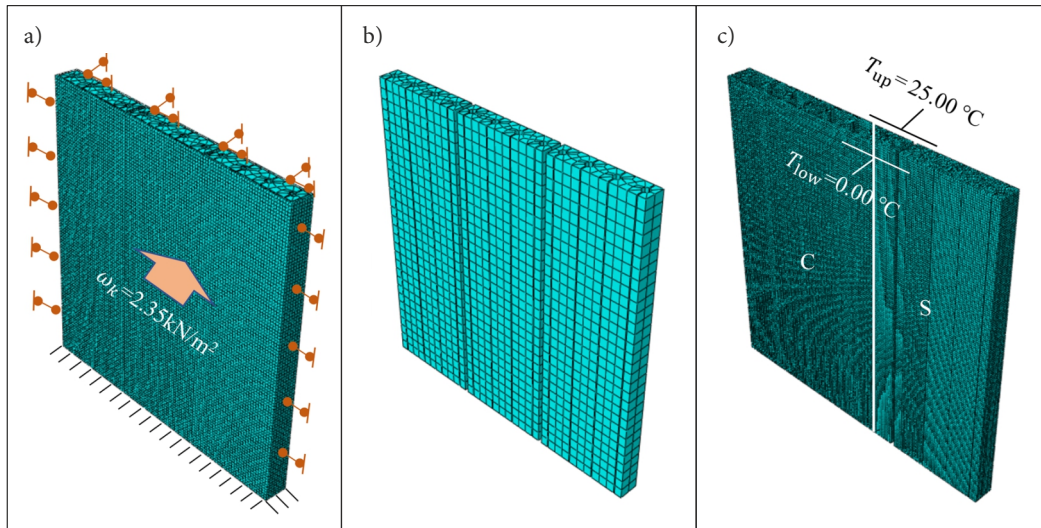


Figure 4. Boundary conditions and mesh of VBEPsc: a – boundary and load conditions, ω_k is the standard wind load on VBEPsc; b – the mesh of straw filler in the mechanical model; c – the mesh of concrete (left) and straw filler (right) in the heat transfer model

door and outdoor temperature in winter is simulated, and the preset temperature is 0 °C for the outer surface and 25 °C for the inner surface. The four edge sides were identified as ideal heat-isolated surfaces which makes the heat flow follows the temperature gradient in a one-dimensional behavior. The values of thermal conductivity of concrete and straw are taken as shown in Table 2. It is assumed that the temperatures of the contact surfaces of both are the same, so tie constraints are used. There are few cavities (air content) in straw with high density (250 kg·m⁻³), which leads to weak thermal radiation and convection, so only solid heat transfer is considered and equates straw to a uniform solid with uniform thermal conductivity. Figures 4a, 4b, and 4c show the boundary conditions and meshing of the heat transfer analysis model using VBEPsc as an example.

3. Results and discussion

3.1. Comparative performance analysis of four types of BEPs with previously reported structural parameters

The stress distribution and numerical results of the mechanical and heat transfer properties of the four BEPs, whose core structure maintained the optimal parameters from the original texts (Zhang et al., 2019, 2020a; Hu, 2021; Hu et al., 2021) and whose conformation dimensions were unified, are shown in Figures 5 and 6. The corners of TBEPsc with the highest stress magnitude are marked by black arrows in Figure 5d. First, the mechanical properties were analyzed. Since the maximum deflection² of each plate in the analytical results remained less than 0.12 mm, which

is 1/10 of its limit (12 mm), only the maximum von Mises stress and maximum principal tensile stress are given in Figure 6a. The stress distribution is shown in Figure 6. Both stress increase in the following order, namely, IBEPsc, VBEPsc, EBEPsc, and TBEPsc, while the mechanical properties decrease sequentially in the same order. This phenomenon can be explained intuitively from the magnitude of the out-of-plane bending moment of inertia (denoted as I_x) of each BEP. Under the aforementioned constraints, the maximum stress in the model is controlled by I_x , which is determined by the reinforcing ribs, the compartmentalization effect of the core structure (mainly the honeycomb walls), and the load-bearing configuration formed with the outer panel. The “I” beam in the IBEPsc (web thickness 20 mm) formed by continuous honeycomb walls parallel to the bending direction and panels has the maximum equivalent I_x . Due to the lower contribution of vertical columns located near the neutral axis to I_x , the load-bearing configuration in VBEPsc can also be considered an “I” beam (web thickness 10 mm), whose equivalent I_x ranks second. Similar “I” beams (web thickness 20 mm) at an angle of 30° to the bending direction are formed in the hexagonal honeycomb wall of the EBEPsc, but the offset of adjacent microelements weakens the constraint and makes its I_x rank third. Finally, only dotted concentration restraints and “I” short elements are formed at the intersection of the outer panels and trabeculae. The absence or scarcity of reinforcing ribs and the compartmentalization effect render the I_x of the TBEPsc the lowest. For the difference between the stress magnitudes and the limit values, it is found that the maximum von Mises stress (dashed line in Figure 6a) is much less than the limit value (4.29 MPa), which means that they all meet the bearing capacity requirement. The maximum principal tensile stress (solid line in Figure 6a) is closer to the limit value (1.43 MPa); specifically, that of TBEPsc reaches 1.69 MPa and fails to meet the serviceabil-

² The maximum deflection deformation in the original TBEPsc model (Zhang et al., 2019) has a clerical error, and thus the correct spelling can be found in this paper.

ity requirement. Thus, it can be concluded that the maximum principal tensile stress is the controlling index for determining the mechanical properties of the four BEPs.

Then, the heat transfer insulation performance was investigated. According to the histogram of Figure 6b, the minimum heat transfer coefficient is $0.92 \text{ W}\cdot\text{m}^{-2}\cdot\text{K}^{-1}$ for TBEPsc, and the maximum is $1.11 \text{ W}\cdot\text{m}^{-2}\cdot\text{K}^{-1}$ for EBEPsc. They all satisfy the self-insulation requirement (less than

$1.5 \text{ W}\cdot\text{m}^{-2}\cdot\text{K}^{-1}$). A proportional relationship is found between the heat transfer coefficient and the core concrete area, except for VBEPsc. This can be explained by the thermal bridging effect, which has been previously elucidated; the heat flux is mainly transferred through the core concrete connecting the outer panels (Zhang et al., 2020a). The nonproportional relationship between the minimum core concrete area (10 mm thick honeycomb wall) and

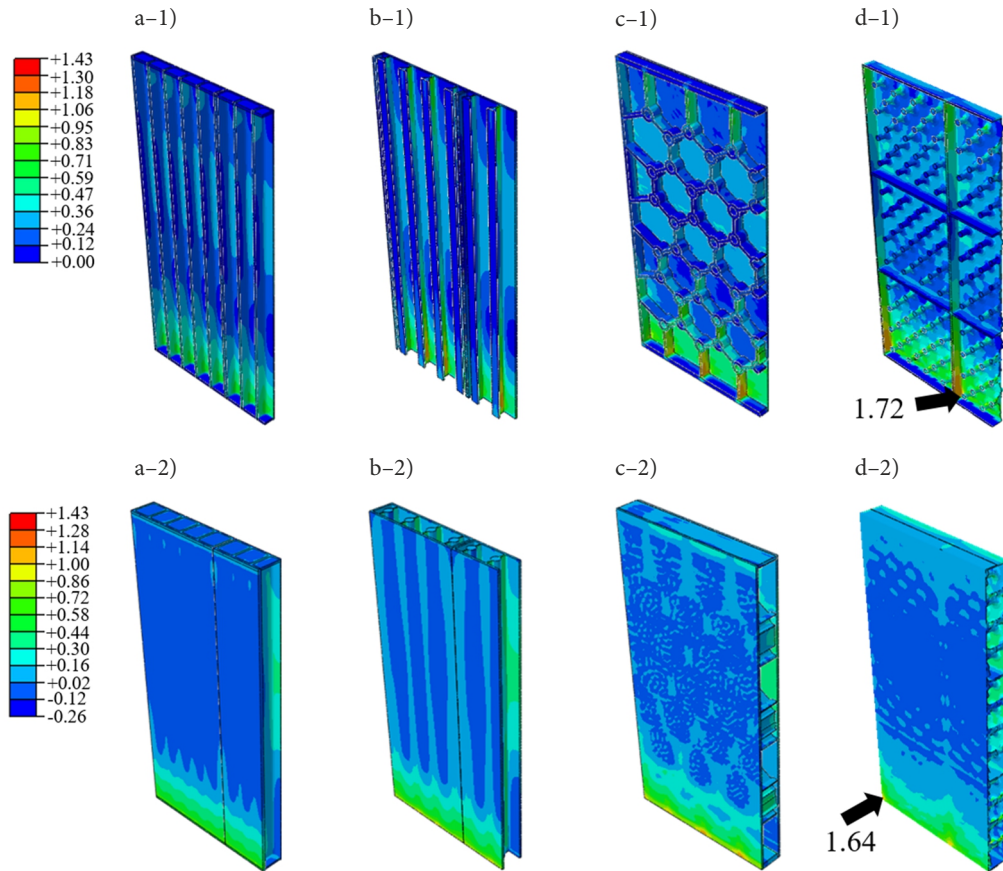


Figure 5. The von Mises stress (-1) and maximum principal stress (-2) contours of four BEPs: a – IBEPsc; b – VBEPsc; c – EBEPsc; d – TBEPsc (MPa)

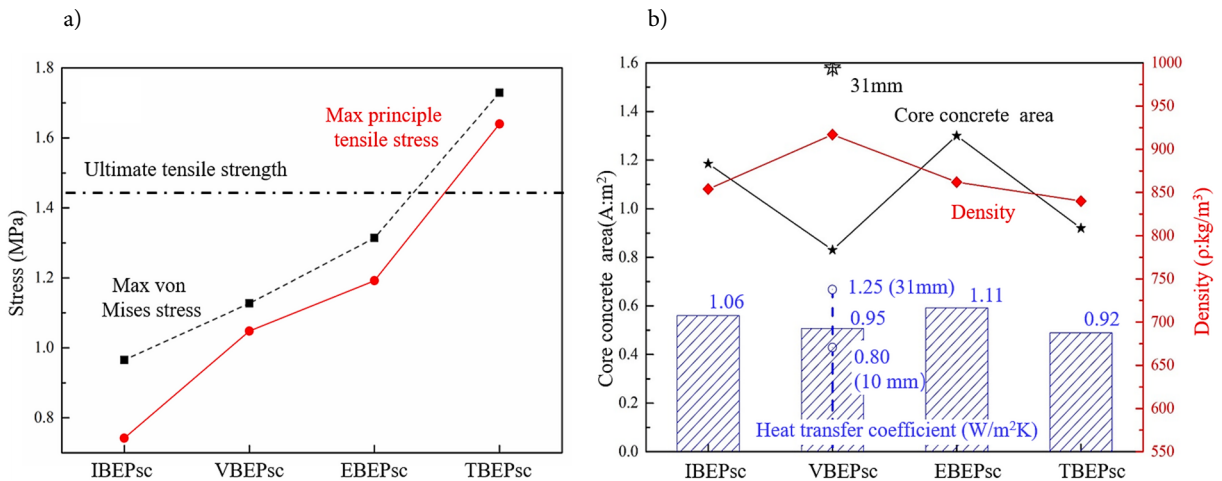


Figure 6. Performance comparison of the four BEPs: a – maximum von Mises stress and maximum principal tensile stress; b – Heat transfer coefficient, core concrete area (left axis), and equivalent density (right axis)

the second smallest heat transfer coefficient of the VBEPsc is due to the nonuniform core structure with the highest equivalent density (diamonds in Figure 6b), which has a significant effect on the heat transfer performance. To specify the effect, two more models with uniform honeycomb walls were tested. Their wall thicknesses were 10 mm and 31 mm, which were determined by deleting the vertical trabeculae or evenly distributing their volumes. Their heat transfer coefficients were 0.80 and $1.25 \text{ W}\cdot\text{m}^{-2}\cdot\text{K}^{-1}$, which are 15% lower and 32% higher than those of VBEPsc. The expanded part in the middle of the nonuniform section will intensify the thermal bridge effect and increase the heat transfer coefficient despite the smallest section on both ends. The results reveal not only the decisive role of the minimum section in heat transfer but also, more importantly, the possibility of achieving the best heat transfer and mechanical properties by optimizing the nonuniform section in future studies. It is also possible to prefabricate BEPs with properties that best meet engineering requirements by designing the cross-section of the core layer, promoting diversification and applicability. This is an interesting research direction with practical value.

In summary, regarding the mechanical and thermal insulation properties of the four BEPs with the reported structural parameters, IBEPsc is most suitable for nonload-bearing walls. At the same time, as research studies progress, further optimized countermeasures are available for the aforementioned weakest mechanical properties of the TBEPsc and thermal insulation properties of the EBEPsc. In the following section, the structures of these two models are further improved to fully explore their structural advantages. A property comparison was conducted again to determine the differences between the four BEPs containing new models.

3.2. Further optimization of TBEPsc and EBEPsc and comprehensive analysis of the four models

In this section, a comprehensive analysis of the four models is given after the strategies for further optimization of the TBEPsc and EBEPsc are conducted and their updated performances are stated.

3.2.1. Strategies and results of further optimization of TBEPsc and EBEPsc

To overcome the weaknesses of the mechanical properties of the TBEPsc and the insulation properties of the EBEPsc, the following optimization or improvement strategies were adopted after analyzing the correlation between the structural characteristics of the core layer and weak properties. Their simulation results are subsequently elaborated.

The weak bearing capacity of TBEPsc is attributed to the scarce I_x supplied by the dotted concentration restraint and discontinuous "l" short elements. Therefore, by optimizing the solid trabeculae in the TBEPsc to hollow trabeculae, the dotted restraints are converted to ring reinforced ribs. The edge panel of the 1×1 m model is kept as a honeycomb wall in the 3×3 m model (still denoted as TBEPsc, Figure 7a). In this way, the continuity of bearing elements, the magnitude of equivalent I_x , the compartmentalization effect, and the uniformity of the constraint distribution are improved simultaneously. Therefore, with regard to the optimal structural parameters of the TBEPsc with solid trabeculae, the mechanical and heat transfer properties of the 1×1 m TBEPsc models with trabecula inner radii of 30, 40, 50, and 60 mm, trabecula spacings of 240, 250, 260 and 270 mm, and trabecula wall thicknesses of 20 mm were solved by using the finite element method. Since a column spacing higher than 270 mm results in a narrow distance between the edge columns and the outer panels (less than 20 mm), which is not conducive to construction, a larger column spacing is not considered. Considering the mechanical and heat transfer properties, an inner diameter of 80 mm and a trabecula spacing of 270 mm were determined to be the most suitable parameters. For the performance of the 3×3 m main scale model, the maximum principal tensile stress was reduced from 1.69 MPa to 1.09 MPa by 35.5%, while the heat transfer coefficient increased from 0.96 to $1.49 \text{ W}\cdot\text{m}^{-2}\cdot\text{K}^{-1}$ due to the significant increase in the amount and cross-sectional area of the core concrete.

For the EBEPsc, although its hexagonal honeycomb wall can provide a multidirectional bending moment of inertia to cope with compound stress, it is not dominant in

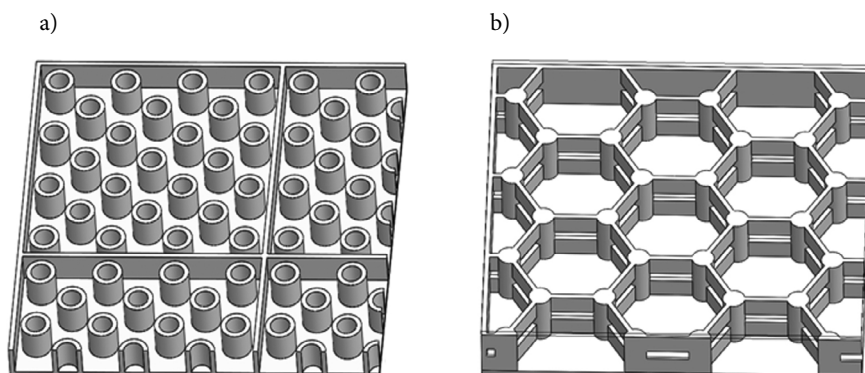


Figure 7. Further optimized beetle elytron plates: a – TBEPsc; b – EBEPsc

the one-way slab condition. Conversely, the higher amount and cross-sectional area of the core concrete weakened its insulation properties. It is noted that the bearing element in the EBEPsc is "I" shaped, and the contribution of the material to the moment of inertia shows a characteristic of being high far from the neutral axis and low near the neutral axis. This means that after the concrete near the neutral axis of the honeycomb wall is removed, the bearing element can still maintain a moment of inertia similar to what it was before. Therefore, to reduce the amount and cross-sectional area of the core concrete and improve the insulation performance of the EBEPsc, the honeycomb walls of the EBEPsc are designed as hollow structures with a gap in the middle, as shown in Figure 7b. Then, separated honeycomb walls form a double T-shaped section with the outer panels. In this way, the mechanical properties of the EBEPsc can be maintained while truncating the heat transfer path of the core concrete and improving the thermal bridge effect, which is an application of the aforementioned nonuniform section optimization method. It should be noted that the prominent stress concentration on the cylinder wall of the hollow column would be observed if the trabecula remained hollow in the finite element analysis. Therefore, the original hollow trabeculae with internal and external diameters of 88/128 mm were replaced with 88 mm diameter solid trabeculae (Figure 7b). Two parameters, the column spacing and the height of the gap are optimized to improve the thermal insulation performance. While ensuring that the mechanical performance still meets the requirements, the amount of concrete is also reduced as much as possible. The mechanical and heat transfer properties of 3×3 m EBEPsc with gap heights of 20, 30, 40, and 50 mm and column spacings of 250, 255, and 265 mm are calculated. Considering the out-of-plane bending resistance and thermal insulation performance, the column spacing and gap height are determined to be 255 mm and 30 mm, respectively. After further optimization, the maximum principal tensile stress of the EBEPsc slightly increased from 1.19 MPa to 1.35 MPa

by 13.45%, while the thermal insulation performance improved and the heat transfer coefficient decreased from $1.11 \text{ W} \cdot \text{m}^{-2} \cdot \text{K}^{-1}$ to $0.90 \text{ W} \cdot \text{m}^{-2} \cdot \text{K}^{-1}$ by 23.33%.

3.2.2. Comprehensive analysis of the four models

To facilitate comparison, the final results of the four BEPsc models, after further optimization of TBEPsc and EBEPsc was conducted, are given in Figure 8, where the performances of TBEPsc and EBEPsc before optimization are marked in scatter form. Accordingly, it can be seen that the maximum principal tensile stress of TBEPsc with hollow trabeculae decreases by 33.53% and indeed drops below the limit value. However, the significant increase in the amount of concrete (maximum density, rhombus in Figure 8b) and the core concrete area increases the heat transfer coefficient by 55.0% to $1.49 \text{ W} \cdot \text{m}^{-2} \cdot \text{K}^{-1}$, which becomes the largest value and is already quite close to the limit value of the self-insulation requirement ($1.5 \text{ W} \cdot \text{m}^{-2} \cdot \text{K}^{-1}$). The heat transfer coefficient of the EBEPsc with separated honeycomb walls decreases by 23.33%, but the main tensile stress increases by 13.45% to 1.35 MPa, which is still lower than the limit value of 1.43 MPa. Therefore, after further optimization, the comprehensive performance of TBEPsc is still the weakest among the four BEPsc, with EBEPsc and VBEPsc in the middle level. However, both the complex structure of the EBEPsc and the 10 mm honeycomb walls in the VBEPsc, which are too thin for walls with typical dimensions of 2–3 m long, are difficult to manufacture. Finally, the IBEPsc is best suited as a straw-filled BEP nonload-bearing wall due to its best comprehensive mechanism and thermal insulation performance, smaller amount of concrete (low density), and simple structure.

It should be noted that although the original weakest mechanical property of the TBEPsc and the weakest insulation property of the EBEPsc models were significantly improved after promoting the strategies of further optimization, another index fell back into the weakest state. In particular, the heat transfer coefficient of TBEPsc

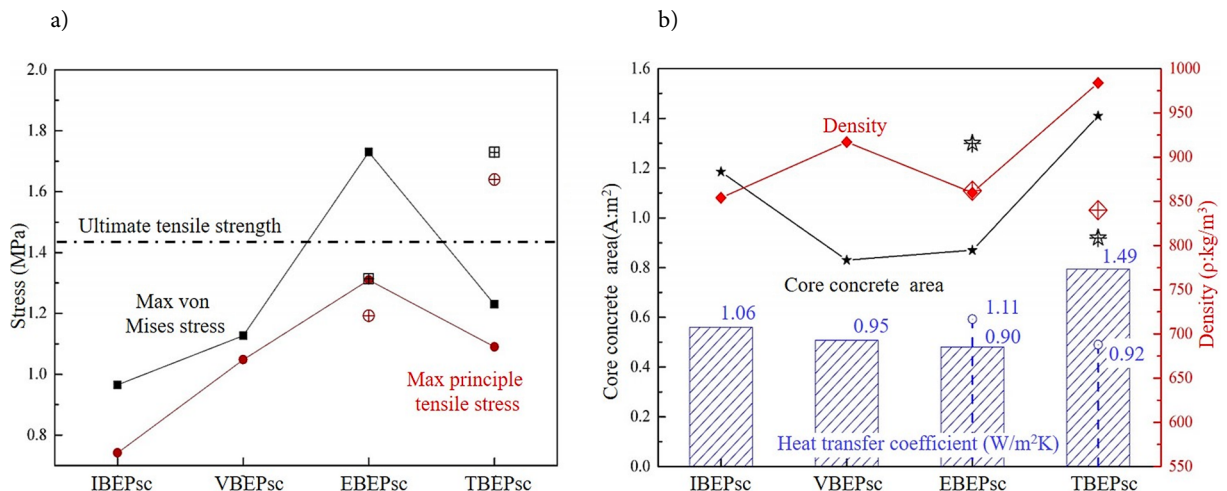


Figure 8. Comparison of the four BEPs after further optimization: a – maximum von Mises stress and maximum principal tensile stress; b – heat transfer coefficient, core concrete area (left axis), and equivalent density (right axis)

is not only the largest but also already quite close to the limit value. Therefore, it can be said that the ranking of the comprehensive performance of the four models is not changed by further optimization. However, there are still the following important implications for further optimization and comparative analysis. 1) The possibility of TBEPsc and EBEPsc having better performance than IBEPsc as a one-way slab after further optimization is removed. Although the panel thickness in this study (240 mm), which is unified to ensure the comparability of the result, is slightly different from the original panel thicknesses of BEPs, it still matches the optimal structural parameters of their core layer. After further optimization and comprehensive analysis of the four models, it is fully confirmed that TBEPsc and EBEPsc still have drawbacks as straw-filled BEP nonload-bearing walls, while IBEPsc is indeed the one with the best comprehensive performance among the four models. Thus, this study provides direct guidance for the selection of beetle boards in engineering. 2) Although the stresses after further optimization of EBEPsc are the largest among the four models, there is still a large gap between their magnitude and the limit value. The insulation performance is improved considerably. In addition, the potential of hexagonal honeycomb walls could not be expressed thoroughly in the one-way slab condition of nonload-bearing walls. However, the complex structure could guarantee excellent mechanical properties rather than disadvantages in compound stress states, such as hollow floors (two-way slabs). In other words, the EBEPsc with reinforcement arranged in outer panels and trabeculae, by combining it with void formers including straw-filled formers and inflatable formers (Void former, n.d.), is expected to be a straw-filled biomimetic hollow floor with excellent mechanical and self-insulation properties. This highlights the direction for the development of load-bearing BEPsc members with outstanding thermal insulation properties. 3) Recently, various biomimetic models have emerged, with dozens of biomimetic models for the three-dimensional structure of beetle forewings alone in this highly specialized field (Jiang et al., 2019; Zhang et al., 2018, 2020b; Chen et al., 2021b). Furthermore, there is a trend of accelerating emergence of new models. However, rare studies have discussed the advantages of new models compared to outstanding models in the same category. Therefore, while continuing to report new biomimetic models, it is also necessary to carry out a parallel comparison with existing models to identify or screen out truly outstanding structures. It can not only discover the optimal structural model for engineering applications but also expose unsolved problems or parts that can be further optimized in existing models, providing direction for the development of even better models.

4. Conclusions

A parallel comparison of the mechanical and thermal insulation properties of four BEP nonload-bearing walls is conducted in this study, and further optimization is carried out for TBEPsc and EBEPsc with weaker properties. Then, the comprehensive performance and the importance of further optimization are clarified, and the following conclusions are obtained:

1. The mechanical properties of BEPsc depend on the maximum principal tensile stress and decrease in the order of IBEPsc, VBEPsc, EBEPsc, and TBEPsc. It is mainly affected by the moment of inertia I_x of each model. For the thermal insulation property, TBEPsc is the best ($0.92 \text{ W}\cdot\text{m}^{-2}\cdot\text{K}^{-1}$), and EBEPsc is the weakest ($1.11 \text{ W}\cdot\text{m}^{-2}\cdot\text{K}^{-1}$). In nonuniform honeycomb walls, the heat transfer coefficient mainly depends on the minimum section area and is affected by the thermal bridge effect caused by the expanded part. According to this, a biomimetic design method is proposed to pursue optimal mechanical and thermal insulation performance through a nonuniform cross-sectional honeycomb wall.
2. The structures of TBEPsc and EBEPsc were further optimized, and their weak performances were significantly improved. However, as another index falls back into the weakest state, the comprehensive performance ranking remains unchanged: TBEPsc is the weakest, EBEPsc and VBEPsc are in the middle, and IBEPsc is the best. In particular, the features of a simple manufacturing process and low cost make IBEPsc most suitable for exterior walls. In addition, the EBEPsc is expected to be applied in load-bearing fields such as hollow floors by combining with steel bars by virtue of hexagonal honeycomb walls suitable for complex force states and mechanical and thermal properties that are far from the limit.
3. With the emergence of various biomimetic models, it is more meaningful to screen for truly outstanding models through parallel comparisons with existing models than to blindly explore new models. This not only helps to discover the optimal structural models for engineering applications but also facilitates learning from the shortcomings of poorly performing models, ensuring that research and development strategies are correct and efficient. From this perspective, this paper also plays a positive guiding and demonstrative role.

Funding

This work was supported by the Fundamental Research Funds for the Central Universities [No. 2242022k30030].

Disclosure statement

The authors declare that they have no known competing financial interests or personal relationships that could have appeared to influence the work reported in this paper.

References

- Bao, P., Ma, S., Han, X., Zhong, S., Fu, H., & Yue, J. (2017). Performance analysis of the ceramsite concrete sandwich insulation composite wallboard. *Journal of Henan University (Natural Science)*, 47(5), 591–596 (in Chinese).
- Chen, J. X. (2018). Twenty years of applied basic research on beetle forewing mimicry: Internal structure, model and its integrated honeycomb plate. *Scientia Sinica Technologica*, 48(7), 701–718 (in Chinese).
<https://doi.org/10.1360/N092017-00208>
- Chen, J. X., Ni, Q. Q., Iwamoto, M., & Endo, Y. (2002). Distribution of trabeculae and elytral surface structures of the horned beetle, *allomyrina dichotoma* (linné) (coleoptera: scarabaeidae). *Insect Science*, 9(1), 55–61.
<https://doi.org/10.1111/j.1744-7917.2002.tb00143.x>
- Chen, J. X., Gu, C., Guo, S., Wan, C., Wang, X., Xie, J., & Hu, X. (2012). Integrated honeycomb technology motivated by the structure of beetle forewings. *Materials Science & Engineering: C*, 32(7), 1813–1817.
<https://doi.org/10.1016/j.msec.2012.04.067>
- Chen, J., Cui, Q., & Ji, Z. (2019a). Thermal insulating performance of multi-layer composite straw wall panel. *Building Energy Efficiency*, 47(4), 64–67 (in Chinese).
- Chen, J. X., Zhang, X. M., Okabe, Y., Xie, J., & Xu, M. Y. (2019b). Beetle elytron plate and the synergistic mechanism of trabecular honeycomb core structure. *Science China Technological Sciences*, 62(1), 87–93.
<https://doi.org/10.1007/s11431-018-9290-1>
- Chen, J., Mohamed Adam Elbashiry E., Yu, T., Ren, Y., Guo, Z., & Liu, S. (2021a). Research progress of wheat straw and rice straw cementbased building materials in China. *Magazine of Concrete Research*, 70(2), 84–95.
<https://doi.org/10.1680/jmacr.17.00064>
- Chen, J. X., Hao, N., Zhao, T. D., & Song, Y. H. (2021b). Flexural properties and failure mechanism of 3D-printed grid beetle elytron plates. *International Journal of Mechanical Sciences*, 210, 106737. <https://doi.org/10.1016/j.ijmecsci.2021.106737>
- Hu, L. (2021). *Study on statics and thermal insulation performance of straw sandwich concrete beetle elytron plate wallboards*. Southeast University.
- Hu, L., Zhang, Z., Chen, J., & Ren, H. (2021). Structural and thermal performance of a novel form of cladding panel – the I-beam beetle elytron plate. In *Proceedings of the Institution of Civil Engineers-Structures and Buildings*.
<https://doi.org/10.1680/jstbu.21.00043>
- Jin, J. (2019). Analysis of China's building energy consumption trends and energy-saving priorities. *Green Environmental Protection Build Materials*, 11, 34–37 (in Chinese).
<https://doi.org/10.16767/j.cnki.10-1213/tu.2019.11.023>
- Jiang, B., Tan, W., Bu, X., Zhang, L., Zhou, C., Chou, C. C., & Bai, Z. H. (2019). Numerical, theoretical, and experimental studies on the energy absorption of the thin-walled structures with bio-inspired constituent element. *International Journal of Mechanical Sciences*, 164, 105173.
<https://doi.org/10.1016/j.ijmecsci.2019.105173>
- Li, H., Dai, M. W., Dai, S. L., & Dong, X. (2018). Current status and environment impact of direct straw return in China's cropland – A review. *Ecotoxicology and Environmental Safety*, 159, 293–300 (in Chinese).
<https://doi.org/10.1016/j.ecoenv.2018.05.014>
- Qing, X., Zhang, G. (2016). Development and engineering application of sintered composite insulation blocks. *Wall Materials Innovation & Energy Saving in Buildings*, 6, 35–38 (in Chinese).
<https://doi.org/10.3969/j.issn.1006-9135.2016.06.038>
- Standardization Administration of China. (2012). *Load code for design of building structures* (GB 50009) (in Chinese).
- Standardization Administration of China. (2015). *Design standard for energy efficiency of public buildings* (GB 50189) (in Chinese).
- Song, Y., Chen, J. S., Chen, J. X., Qin, W. H., Liu, D. Y., & Chen, J. (2021). Extraction and reconstruction of a beetle forewing cross-section point set and its curvature characteristics. *Pattern Analysis and Application*, 25, 77–87.
<https://doi.org/10.1007/s10044-021-01037-0>
- Void Former. (n.d.). <http://www.jj-txhb.com/>
- Wu, C., Liu, F., Fan, J., & Wu, Y. (2015). Research on the heat transfer performance of I-shaped self-insulation concrete block wall filling with compressed blocks of straw. *Concrete*, 6, 127–130 (in Chinese). <https://doi.org/10.3969/j.issn.1002-3550.2015.06.034>
- Xu, M. Y., Pan, L. C., Chen, J. X., Zhang, X. M., & Yu, X. D. (2019). The flexural properties of end-trabecular beetle elytron plates and their flexural failure mechanism. *Journal of Materials Science*, 54(11), 8414–8425.
<https://doi.org/10.1007/s10853-019-03488-7>
- Yu, T., Ren, Y., Guo, Z., Chen, X., & Chen, J. (2021). Progress of research on cotton and corn straw cement-based building materials in China. *Advances in Cement Research*, 30(3), 93–102.
<https://doi.org/10.1680/jadcr.17.00040>
- Zhang, X. M., Xie, J., Chen, J. X., Okabe, Y., Pan, L. C., & Xu, M. Y. (2017). The beetle elytron plate: A lightweight, high-strength and buffering functional-structural bionic material. *Scientific Reports*, 7(1), 4440.
<https://doi.org/10.1038/s41598-017-03767-w>
- Zhang, L., Bai, Z., & Bai, F. (2018). Crashworthiness design for bio-inspired multi-cell tubes with quadrilateral, hexagonal and octagonal sections. *Thin-Walled Structures*, 122, 42–51.
<https://doi.org/10.1016/j.tws.2017.10.010>
- Zhang, Z., Chen, J., Mohamed Adam Elbashiry, E., Guo, Z., & Yu, X. (2019). Effect of changes in the structural parameters of bionic straw sandwich concrete beetle elytron plates on their mechanical and thermal insulation properties. *Journal of the Mechanical Behavior of Biomedical Materials*, 90, 217–225.
<https://doi.org/10.1016/j.jmbbm.2018.10.003>
- Zhang, Z., Mohamed Adam Elbashiry, E., Chen, J., Wei, P., & Fu, Y. (2020a). Optimization of the structural parameters of the vertical trabeculae beetle elytron plate based on mechanical and thermal insulation properties. *KSCE Journal of Civil Engineering*, 24(12), 3765–3774. <https://doi.org/10.1007/s12205-020-2334-x>
- Zhang, X. M., Yu, X. D., Chen, J. X., Pan, L. C., Hu, L. P., & Fu, Y. Q. (2020b). Vibration properties and transverse shear characteristics of multibody molded beetle elytron plates. *Science China Technological Sciences*, 63(12), 2584–2592.
<https://doi.org/10.1007/s11431-019-1570-6>